MOLECULAR IMAGING AND BIOLOGY

Mol Imaging Biol (2015) 17:185–194
DOI: 10.1007/s11307-014-0792-6

Published Online: 2 October 2014

RESEARCH ARTICLE

Optimization of Mesenchymal Stem Cells (MSCs) Delivery Dose and Route in Mice with Acute Liver Injury by Bioluminescence Imaging

Zhengran Li,[1] Xiaojun Hu,[1] Junjie Mao,[1] Xuelian Liu,[1] Lina Zhang,[1] Jingjing Liu,[1] Dan Li,[1] Hong Shan[1,2]

[1]*Department of Radiology, The Third Affiliated Hospital of Sun Yat-sen University, Guangzhou, 510630, China*
[2]*Interventional Radiology Institute, Sun Yat-sen University, Guangzhou, 510630, China*

Abstract

Purpose: Both experimental and initial clinical studies have shown the therapeutic potential of mesenchymal stem cells (MSCs) in liver disease. Noninvasive tracking of MSCs could facilitate its clinical translation. The purpose of this study was to optimize MSCs delivery dose and route in mice with acute liver injury using bioluminescence imaging (BLI) to track the cells.

Procedures: MSCs were labeled with the Luc2-mKate2 dual-fusion reporter gene (MSCs-R). The fate of MSCs-R was tracked through *in vivo* BLI after administration of different doses or delivery through different routes.

Results: When delivered *via* the superior mesenteric vein (SMV), the high-dose (1.0×10^6 and 5.0×10^5) group mice demonstrated high liver BLI signal but also had lethal portal vein embolization (PVE). By contrast, no PVE and its related death occurred in the low-dose (2.5×10^5) group mice. Thus, 2.5×10^5 is the optimal delivery dose. Three delivery routes, i.e., inferior vena cava (IVC), SMV, and intrahepatic (IH) injection, were also systematically compared. After IVC infusion, MSCs-R were quickly trapped inside the lungs, and no detectable homing to the liver and other organs was observed. By IH injection, lung entrapment was bypassed, but MSCs-R distribution was only localized in the injection region of the liver. By contrast, after SMV infusion, MSCs-R were dispersedly distributed and stayed as long as 7-day posttransplantation in the liver. The *in vivo* imaging results were further validated by *ex vivo* imaging, digital subtraction angiography (DSA), and tissue analysis. Therefore, SMV is the optimal MSCs delivery route for liver disease.

Conclusions: Collectively, BLI, which could dynamically and quantitatively track cellular location and survival, is useful in determining MSCs transplantation parameters.

Key words: Mesenchymal stem cells, Liver disease, Delivery dose, Delivery route, Bioluminescence imaging

Introduction

Various etiologies such as toxins, drugs, viral infections, immune reactions, or genetic disorders may cause acute or chronic liver injury. Once liver cirrhosis is present, patients have a high incidence of serious complications, including portal hypertension, liver failure, and liver cancer.

Electronic supplementary material The online version of this article (doi:10.1007/s11307-014-0792-6) contains supplementary material, which is available to authorized users.

Correspondence to: Dan Li; *e-mail:* lidan25@mail.sysu.edu.cn, Hong Shan; *e-mail:* shanhong@mail.sysu.edu.cn

Increasing evidence suggests that mesenchymal stem cells (MSCs) transplantation can be a promising treatment for liver disease. MSCs can be obtained from various somatic tissues [1] and show favorable characteristics, such as ease of isolation and expansion, differentiation potential, lack of teratoma formation, and low ethics controversy. MSCs can differentiate into mature hepatocytes *in vitro* under adequate stimuli, such as cytokines and growth factors [2–5], coculture with hepatocytes or nonparenchymal liver cells [6–8], three-dimensional (3D) culture [9, 10], and transcription factor transduction [11]. In liver injury animal models, MSCs not only differentiate into hepatocytes to provide hepatic function [12–14], but also produce a series of bioactive factors that reduce hepatocyte apoptosis and inhibit inflammatory responses [15–17]. Initial studies in humans also predict the potential clinical application of MSCs in the treatment of liver disease [18, 19].

Before broadening the use of MSCs to clinical therapy, variables like cell dose, dosing frequency, delivery route, timing of delivery, and host microenvironment should be defined to ensure safe and effective administration. To satisfy these demands, it is desirable to establish novel molecular imaging methods to longitudinally and noninvasively track cellular fate (i.e., distribution, localization, engraftment, and repopulation) *in vivo* following transplantation. In former studies of liver disease, MSCs were labeled with superparamagnetic iron oxide (SPIO) [20], quantum dots [21], or radionuclides [22], and their distribution was monitored using *in vivo* magnetic resonance imaging (MRI), fluorescence imaging (FLI), or single-photon emission computed tomography (SPECT), respectively. In another study, SPIO and luciferase reporter gene were codelivered into MSCs with polymer-based nonviral vector, and then, cells were tracked using both *in vivo* MRI and bioluminescence imaging (BLI) [23]. The transiently labeled contrast agents or reporter genes are diluted with each cellular division, and therefore are not able to accurately assess cell viability. In this study, MSCs were stably labeled with Luc2-mKate2 dual-fusion reporter gene by lentiviral transduction, and the optimal dose and delivery route for liver disease were determined through *in vivo* BLI in a mouse model.

Materials and Methods

Construction of pLenti-CMV-Luc2-mKate2 and Preparation of MSCs-Luc2-mKate2 (MSCs-R)

Lentiviral expression vector pLenti6.3/V5-DEST carrying Luciferase2 (Luc2, Promega Inc., Madison, WI, USA) and mKate2 (Evrogen Inc., Moscow, Russia) dual-fusion reporter gene was constructed according to the manufacturer's protocol (Invitrogen Inc., Carlsbad, CA, USA). The expression vector (pLenti-CMV-Luc2-mKate2) and ViraPower™ Packaging plasmid Mix were cotransfected into 293FT cells with Lipofectamine 2000 (Invitrogen Inc.). The culture supernatants were collected, concentrated, and used as a virus stock.

The immortalized human bone marrow-derived MSCs UE7T-13 were provided by the RIKEN BioResource Center through the National Bio-Resource Project of the MEXT, Japan. These cells were maintained under standard conditions as described previously [24, 25]. MSCs were infected with pLenti-CMV-Luc2-mKate2 lentivirus with a multiplicity of infection (MOI) of 21 and 8 μg/ml polybrene for 48 h. Through flow cytometry, the percentage of mKate2-positive cells was determined, and positive cells (MSCs-R) were further purified.

Multilineage Differentiation of MSCs-R

To evaluate the effect of the Luc2-mKate2 reporter gene on the multilineage differentiation potential of MSCs, MSCs-R were induced to differentiate into adipogenic, osteogenic, and chondrogenic lineages using STEMPRO® Differentiation Kit (Invitrogen Inc.). After induction, cells were stained with oil red O for lipid droplets, alizarin red S for calcium, or alcian blue for mucopolysaccharides, respectively.

Preparation of Acute Liver Injury Model and MSCs-R Transplantation

Animal procedures were performed according to the protocol approved by the Sun Yat-sen University Institutional Animal Care and Use Committee. Male 6- to 8-week-old athymic nude mice (BALB/c nu/nu) were purchased from Beijing Vital River Laboratory Animal Technology Co. Ltd. (Beijing, China). To prepare acute liver injury model, mice were treated by peritoneal injection of 20 % CCl_4 every other day for two times. The injection dose was 2.5 ml/kg body weight. MSCs-R transplantation was performed at 24 h after the secondary administration of CCl_4.

All operations were performed under anesthesia with 10 mg/ml ketamine and 2 mg/ml xylazine in PBS. Mice underwent aseptic laparotomy. MSCs-R suspended in 0.25 ml saline were transplanted into mice *via* three different routes, including inferior vena cava (IVC), superior mesenteric vein (SMV) [20], and intrahepatic (IH) injection. A 29-gauge needle was used for puncture and injection of cells. The total injection time was no less than 1 min.

In Vitro, In Vivo and Ex Vivo Bioluminescence Imaging

BLI was performed using Xenogen IVIS Lumina II imaging system and analyzed using IVIS Living Imaging 4.2 software (Caliper Life Sciences, Alameda, CA). Bioluminescence images were normalized and reported as photons per second per centimeter squared per steradian (p/s/cm^2/sr). For *in vitro* BLI, 1.0×10^3, 1.25×10^3, 2.5×10^3, 5.0×10^3, 1.0×10^4, 1.25×10^4, 2.5×10^4, 5.0×10^4, and 1.0×10^5 MSCs-R were planted on black 96-well plate. After the incubation of D-luciferin (150 μg/ml), cell bioluminescence signals were detected with an acquisition time of 5 s. For *in vivo* BLI of transplanted MSCs-R, mice were injected with D-luciferin intraperitoneally

at a dose of 150 mg/kg body weight. Bioluminescence signals were detected with the acquisition time of 30 s. For *ex vivo* BLI, mice were euthanized after D-luciferin injection. The major organs were dissected and subjected to *ex vivo* BLI. Bioluminescence signals were detected with the acquisition time of 30 s.

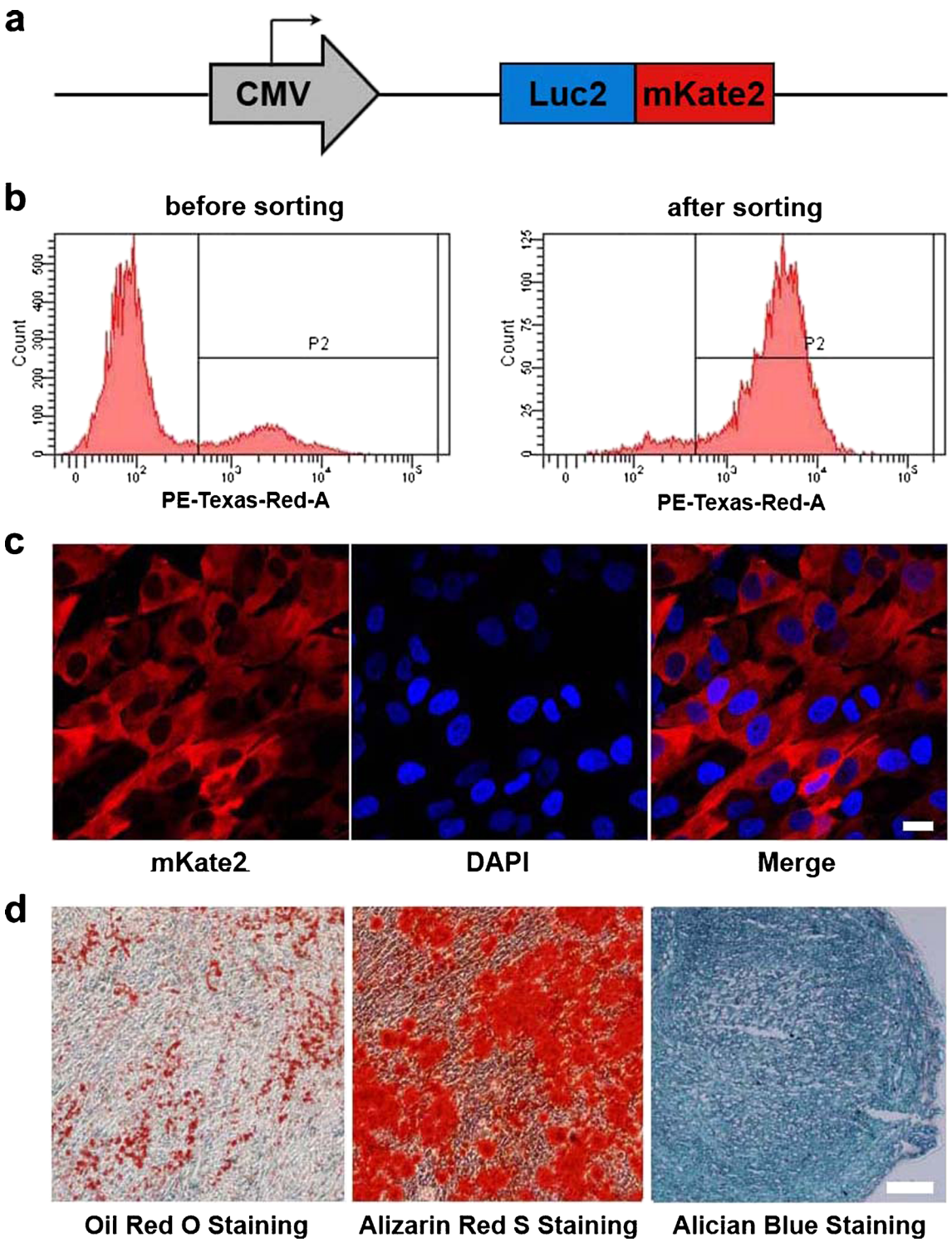

Fig. 1. **a** Schema of lentivirus vector carrying dual-fusion reporter gene (Luc2-mKate2) driven by a constitutive CMV promoter. **b** Flow cytometric analysis of Luc2-mkate2 lentivirus-transduced MSCs before and after fluorescence-activated cell sorting. **c** Confocal analysis of MSCs-Luc2-mKate2 (MSCs-R). *Scale bar*, 20 μm. **d** Assessment of multilineage differentiation ability of MSCs-R. After induction, adipocytes, osteoblasts, and chondrocytes were stained with oil red O, alizarin red S, and alcianblue, respectively. *Scale bar*, 200 μm.

Postmortem Tissue Assay

Postmortem tissue assay was performed as described previously [26–28]. Organs were dissected at 3-day posttransplantation of MSCs-R. Frozen tissue sections (5 μm thick) were fixed for 20 min at room temperature in 4 % paraformaldehyde and subsequently covered with DAPI-containing mounting medium. Images were obtained using fluorescence microscopy.

Statistical Analysis

Quantitative data are expressed as mean±SD. Means were compared using one-way ANOVA and the Student's *t* test. *P* values of <0.05 were considered statistically significant.

Results

Labeling MSCs with Luc2-mKate2 Dual-Fusion Reporter Gene by Lentivirus Transduction

To develop the imaging approach, MSCs were labeled with the Luc2-mKate2 dual-fusion reporter gene by lentiviral transduction. Luc2 can be used for *in vivo* BLI while mKate2 can be used for fluorescence assay at the cellular level *in vitro* and the tissue level *ex vivo*. Luc2 and mKate2 are joined by an 8-amino acid peptide (NRDPPVAT). The dual-fusion reporter gene was driven by a constitutive CMV promoter (Fig. 1a). The labeling efficiency was 17.5 % based on the flow cytometric analysis of mKate2-positive cells (MSCs-R) (Fig. 1b). After fluorescence-activated cell sorting, the percentage of MSCs-R was raised to 92.8 % (Fig. 1b). Confocal analysis of MSCs-R demonstrated uniform mKate2 expression within the cytoplasm (Fig. 1c). MSCs carrying Luc2-mKate2 (MSCs-R) showed similar morphology to nonlabeled MSCs (control). Like control MSCs, MSCs-R were still able to differentiate into adipogenic, osteogenic, and chondrogenic lineages (Fig. 1d).

To confirm that the levels of Luc2 reporter gene activities correlated with cell numbers, MSCs-R were assayed through both *in vitro* and *in vivo* BLI. *In vitro* BLI showed a linear relationship between cell number (1.0×10^3 to 1.0×10^5) and bioluminescence signal (R^2=0.997) (Fig. 2a, b). For *in vivo* BLI, different numbers (1.0×10^4 to 1.0×10^6) of MSCs-R were transplanted into the liver of nude mice *via* the SMV. The blood of SMV flows directly into the hepatic portal vein, and therefore delivers MSCs-R into the liver. BLI was performed at 3-h posttransplantation (PT). As shown in Fig. 2c, d, there is also a robust relationship between cell number and bioluminescence signal of the liver (R^2=0.996). The above results suggest that BLI of Luc2 is a reliable approach to monitor viable transplanted MSCs-R quantitatively.

Determination of the Optimal Delivery Dose of MSCs-R

To determine the optimal delivery dose, different numbers (1.0×10^6, 5.0×10^5, and 2.5×10^5) of MSCs-R were transplanted into the liver of nude mice *via* the SMV. The 1.0×10^6 group mice demonstrated the highest liver BLI signal (Fig. 2c), but also had high PT 24-h mortality (50.0 %, 3/6). Liver histology analysis in Fig. 3 showed large area of necrosis accompanied by infiltrating neutrophils, which was caused by portal vein embolization (PVE).

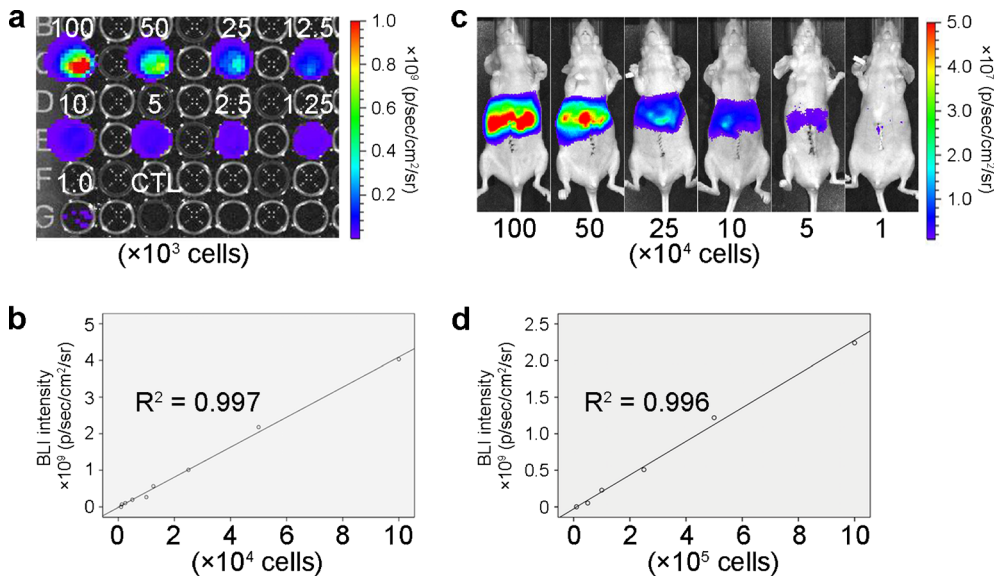

Fig. 2. **a** *In vitro* bioluminescence imaging (*BLI*) of varying numbers of MSCs-R plated on 96-well plate. CTL, control. **b** Linear relationship analysis between the cell number and bioluminescence intensity of **a.** **c** *In vivo* BLI of varying numbers of MSCs-R transplanted into the liver of nude mice *via* superior mesenteric vein (SMV) at 3-h posttransplantation. **d** Linear relationship analysis between the cell number and bioluminescence intensity of **c**.

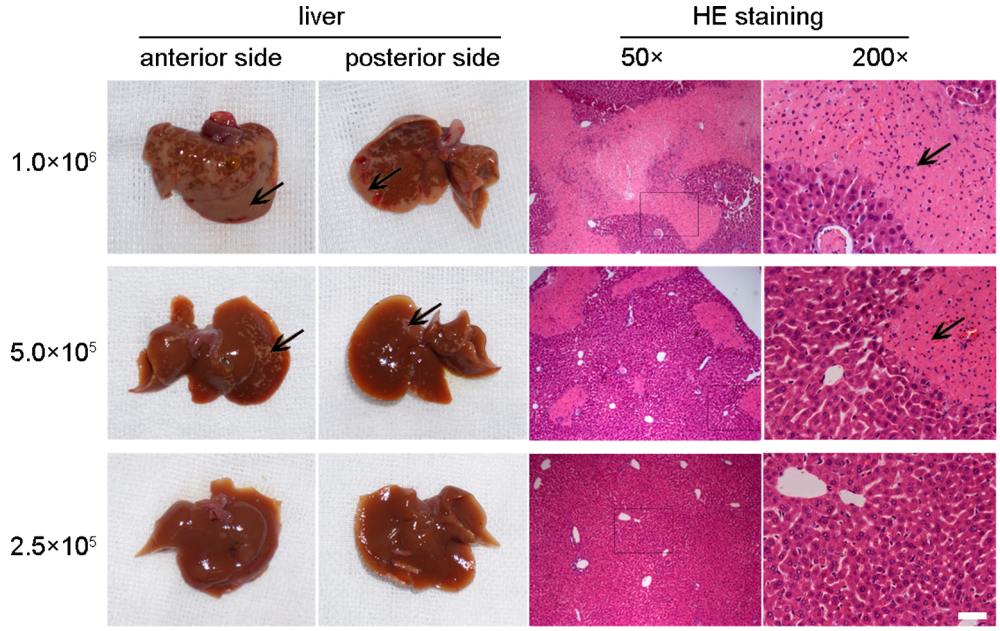

Fig. 3. Appearance and HE staining of the liver 24 h after 1.0×10^6, 5.0×10^5, or 2.5×10^5 of MSCs-R transplanted into the liver of nude mice *via* SMV. *Black arrows* indicate necrotic areas accompanied by infiltrating neutrophils. *Scale bar*, 200 μm.

The 5.0×10^5 group mice had lower 24-h mortality (33.3 %, 1/6) and smaller area of necrosis (Fig. 3). By contrast, no PVE-caused death occurred in the 2.5×10^5 group mice, and histology analysis showed no necrosis in the liver (Fig. 3). Given the above results, 2.5×10^5 is the optimal delivery dose and therefore chosen for further study.

Determination of the Optimal Delivery Route of MSCs-R

To determine the optimal delivery route, 2.5×10^5 MSCs-R were transplanted into acute liver injury model nude mice *via* three different routes, including IVC, SMV, and IH injection. The validity of the acute liver injury model was confirmed through histological assay (Supplementary Material Fig. S1). Representative *in vivo* BLI images and quantifications at different time points PT are shown in Fig. 4a–c. In the IVC group mice, a clear signal can be seen in the lungs at 3-h PT, demonstrating that the majority of infused MSCs-R were trapped inside the pulmonary system. The lung BLI signal declined quickly and reduced to background levels at 7-day PT. However, no BLI signal could be detected in any of the other organs. In the IH group mice, BLI signal was only localized in the injection region of the liver and decreased to background levels at 14-day PT. By contrast, MSCs-R demonstrated dispersed distribution within the liver after SMV transplantation. The liver BLI signal declined progressively with time and retreated to background levels at 10-day PT. No BLI signal could be detected in the lungs or other organs. *Ex vivo* BLI (Fig. 4d, e) further confirmed the *in vivo* BLI results.

To clearly demonstrate MSCs-R migration direction in these three delivery routes, digital subtraction angiography (DSA) was performed on mice (Supplementary Material Fig. S2). In IVC puncture route, blood reentered the heart through the right atrium and went to the lungs through the pulmonary artery. In the SMV puncture route, blood flowed directly into the hepatic portal vein and went to the various hepatic lobes through portal venous branches (Supplementary Material Fig. S2, S3). In the IH puncture route, contrast agent was confined to the injection region of the liver and could not disperse to other regions. The above DSA results were in accordance with the *in vivo* BLI results.

Analysis of MSCs-R Tissue distribution

Fluorescence microscopy analysis of mKate2$^+$ MSCs-R tissue distribution (Fig. 5) was further performed to validate the BLI measurements. In the IVC group, MSCs-R accumulated mainly in the lungs and not in the liver. In the SMV group, MSCs-R were detected to reside in the liver instead of other tissues, including the lungs, heart, kidneys, and spleen (Fig. 5, Supplementary Material Fig. S4). In the IH group, MSCs-R distributed only in the injection region of the liver (Fig. 5) but could not migrate to the noninjection region of the liver (Supplementary Material Fig. S5).

Discussion

Both experimental [12–17] and initial clinical [18, 19] studies have shown the therapeutic potential of MSCs in liver disease. It is of great importance to get direct evidence

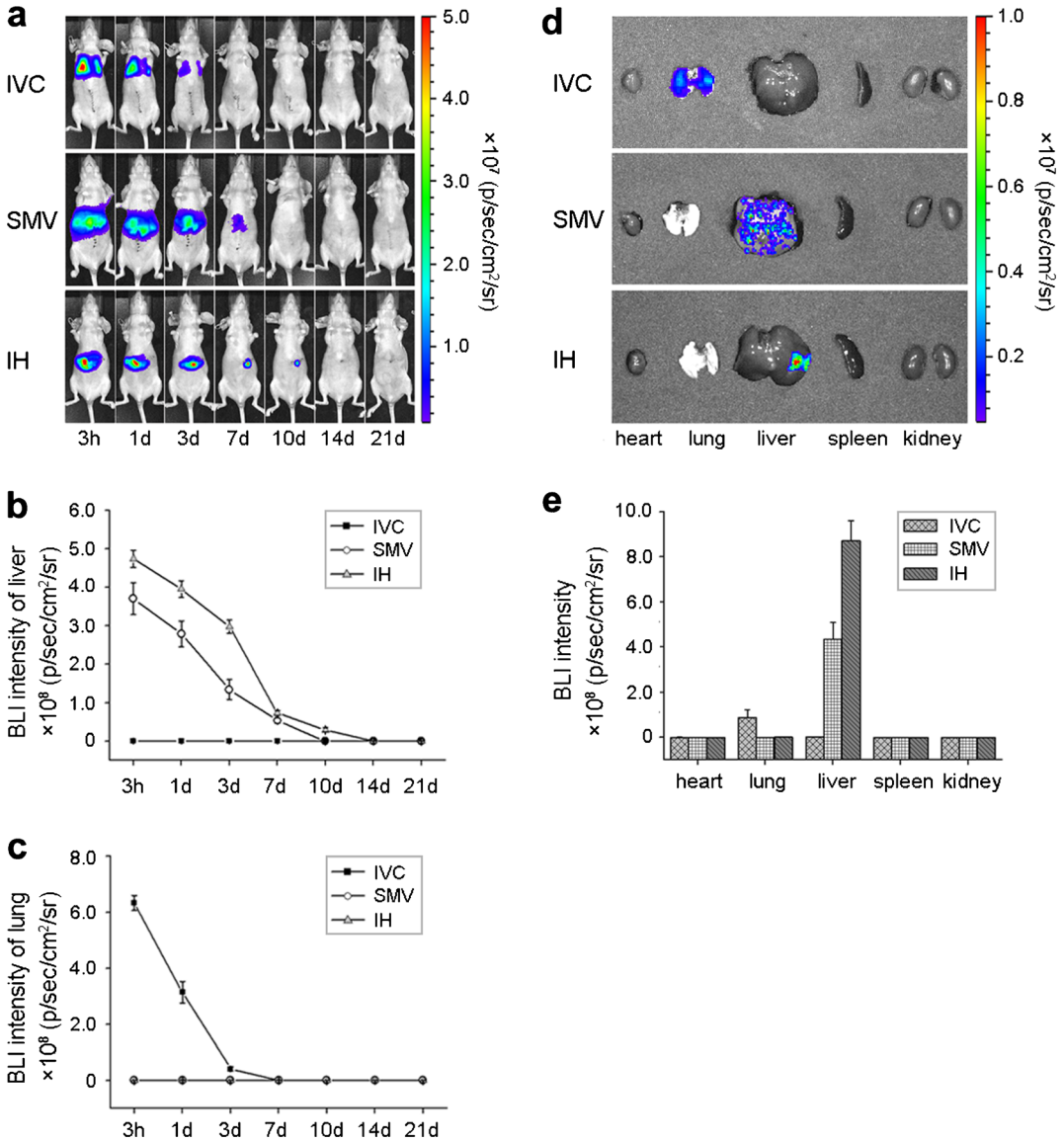

Fig. 4. **a** *In vivo* BLI of acute liver injury model nude mice after transplantation of 2.5×10^5 MSCs-R *via* three different routes, including inferior vena cava (*IVC*), SMV, and intrahepatic (*IH*) injection. **b** Time-liver bioluminescence intensity curves of **a. c** Time-lung bioluminescence intensity curves of **a. d** *Ex vivo* BLI of major organs harvested at 3-day posttransplantation of MSCs-R. **e** Bioluminescence intensity quantification of major organs at 3-day posttransplantation of MSCs-R. All data in **b**, **c,** and **e** are presented as the mean±standard deviation(*SD*).

that transplanted MSCs do survive for enough time and engraft accurately into the injured liver in animal models before initiating clinical applications in humans. Molecular imaging enables *in vivo* cell tracking in a real-time, longitudinal, noninvasive way and could further facilitate assessment, optimization, and guidance of cell transplantation for clinical translation [29, 30].

For cell imaging, cells can be directly labeled with contrast agents such as magnetic particles [20], quantum dots [21], and radionuclides [22] and so on. While direct imaging techniques can be straightforwardly implemented and commonly used, it cannot specifically differentiate viable cells from dead cells because the contrast agents are diluted after every cell division and keep lingering in tissues even after cell death. An alternative approach to cell imaging is reporter gene imaging, which requires the integration of specific reporter genes. This is a favorable imaging technique for long-term assessment of cell survival since its signal generation counts on cell viability. Among various imaging modalities, BLI possesses many advantages including low background, low cost, high sensitivity, no radiation, and simplicity. Thus, it has been widely used in small animal studies. In this study, we use BLI reporter gene for MSCs imaging to determine the optimal delivery dose and route for liver disease.

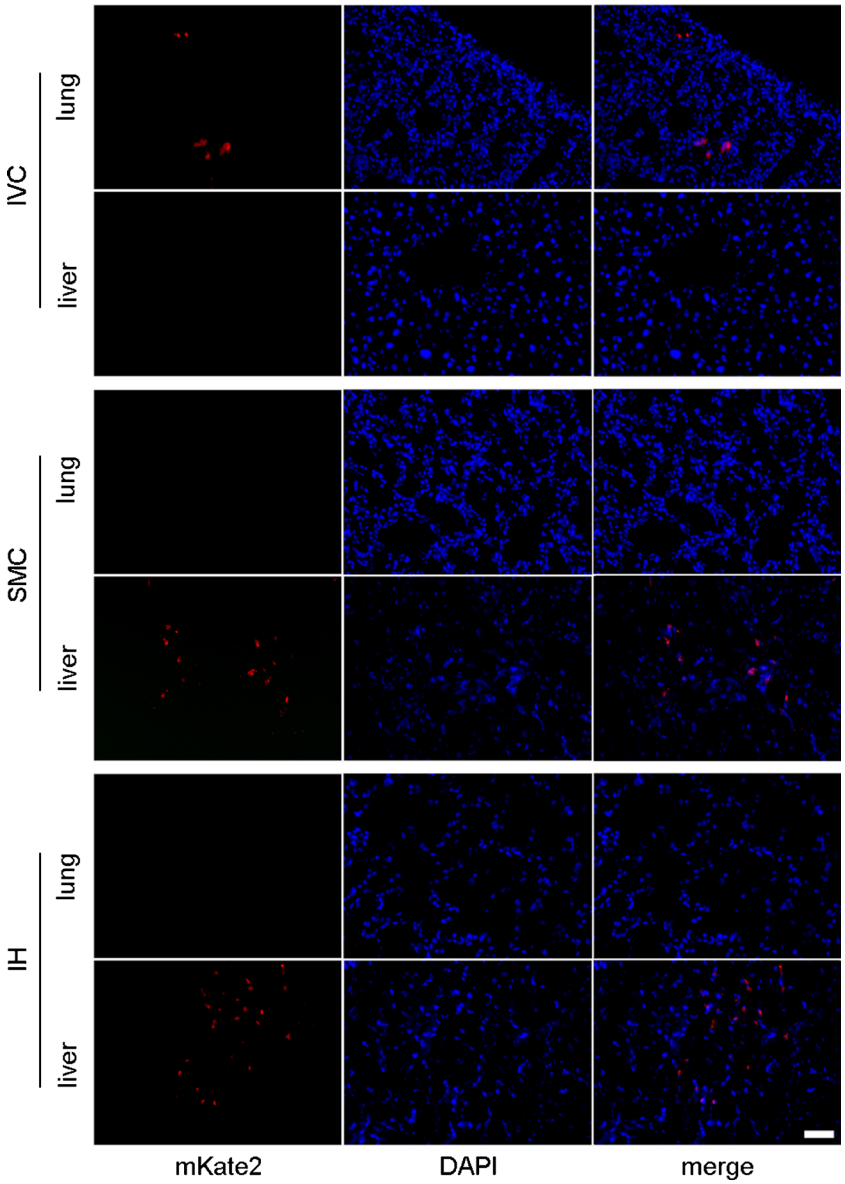

Fig. 5. MSCs-R distribution analysis on lung or liver sections 3-day posttransplantation *via* IVC, SMV, or IH, respectively. *Scale bar*, 100 μm.

In the initial study, the Luc2-mKate2 dual-fusion reporter gene was constructed. Luc2 is a BLI reporter gene, a synthetic firefly luciferase with humanized codon optimization. Compared to wild-type luciferase, Luc2 shows higher expression and reduced abnormal transcription. mKate2 is a far-red fluorescent reporter gene. The brightness of mKate2 is higher compared to any other monomeric fluorescent proteins. Its far-red fluorescence allows high signal-to-background ratio. Besides, it offers excellent pH resistance, high photostability, and low toxicity [31]. The above characteristics of mKate2 make it a superior fluorescent reporter gene. The inclusion of mKate2 is helpful for the cell sorting and tissue analysis. After lentiviral transduction, MSCs-R constitutively express Luc2-mKate2 reporter gene and still keep multileage differentiation ability (Fig. 1). Both *in vitro* and *in vivo* BLI (Fig. 2) show a linear relationship between cell number and bioluminescence signal, which suggests that BLI of Luc2 is a reliable approach to monitor viable transplanted MSCs-R quantitatively.

Delivery dose and route of MSCs are two important parameters that determine therapeutic efficacy. To identify the optimal delivery dose, different numbers (1.0×10^6, 5.0×10^5, and 2.5×10^5) of MSCs-R were transplanted into the liver of nude mice *via* the SMV. The blood from SMV flows directly into the hepatic portal vein, and therefore delivers MSCs-R into the liver. The 1.0×10^6 and 5.0×10^5 group mice demonstrated high liver BLI signal, but also had 50.0 and 33.3 % mortality within 24-h PT, respectively. The death was caused by PVE (Fig. 3). By contrast, no PVE and its related death occurred in the 2.5×10^5 group mice.

Therefore, in order to avoid side effects like PVE, 2.5×10^5 is the optimal dose of MSCs when delivered through the SMV. Lethal pulmonary embolism was also reported after intravenous administration of high-dose MSCs ($1.0–3.0\times10^6$/mouse) [32, 33], likely because MSCs are prone to aggregate in high concentration. One study showed that a combination of MSCs and heparin could avoid pulmonary embolism [33]. Further studies are needed to validate the efficacy of heparin on PVE.

Systemic infusion, portal vein injection, and IH injection are commonly applied MSC delivery approaches for liver disease. Therefore, these three delivery routes were quantitatively compared through *in vivo* BLI in mice with acute liver injury (Fig. 4). Carbon tetrachloride (CCl_4), a potent hepatotoxic agent, was used to induce acute liver injury. Treatment with CCl_4 can cause hepatic steatosis, inflammation, apoptosis, and necrosis through various mechanisms, such as formation of reactive free radicals, induction of hypomethylated ribosomal RNA, and alterations in calcium homeostasis [34]. Peripheral vein (such as tail vein or femoral vein) is the usually used route for systemic infusion. To avoid extravasation at the injection site and ensure the similar level of surgical trauma as the other two routes, systemic infusion of MSCs was implemented through IVC. Portal vein infusion of MSCs was carried out through SMV. After IVC infusion, MSCs-R were quickly trapped inside the lungs and eliminated within 7 days, which is consistent with previous studies [35–37]. However, no detectable homing of MSCs-R to the liver and other organs was demonstrated. Relatively large size and cell surface adhesion molecules might account for the lung entrapment of MSCs [37]. It is reported that MSCs passage through the lung barrier could be significantly increased through prior treatment with vasodilator sodium nitroprusside [35, 36], heparin saturation of MSCs [38], or pronase detachment [39]. Further studies are needed to confirm whether the application of these methods could facilitate MSCs engraftment to the injured liver after systemic infusion. By IH and SMV injection, lung entrapment is bypassed, and MSCs-R were mainly distributed in the liver. Compared to IVC route, these two routes showed higher delivery efficacy to target organ liver and less systemic engraftment, which may reduce side effects. After IH injection, MSCs-R exhibited a longer retention time in the liver than by SMV injection, but their distribution was only localized in the injection region of the liver. In liver disease, the lesion of the liver is usually diffused. In this condition, localized distributed MSCs may execute less efficacious therapy. Also, locally aggregated MSCs are predisposed to establish their own microenvironments [40]. Thus, cautions should be taken when considering direct injection of MSCs into tissues [41]. By contrast, MSCs-R were dispersedly distributed and stayed as long as 7-day PT in the liver after SMV infusion. DSA showed that after SMV puncture, blood flowed directly into the portal vein and went to the various hepatic lobes through portal venous branches (Supplementary Material Fig. S2, S3), which confirmed the *in vivo* BLI results. From the above results, we conclude that the SMV (i.e., portal vein) is the optimal MSCs delivery route for liver disease. In a clinical setting, portal vein puncture is performed through percutaneous transhepatic catheterization [18, 42], which is a minimally invasive intervention surgery. MSCs could also be delivered through artery route. Left ventricular or aortic arch injection is a systematic administration method. When delivered through this route, liver engraftment efficiency of MSCs (less than 10 %) is pretty low [43]. Besides, MSCs are also distributed in other organs, such as the kidney, lung, brain, and heart [43], which may cause side effects. Intra-arterial regional administration, on the other hand, can bypass nonspecific organs and deliver cells directly to the target organs. Therefore, it is often used as delivery route in various disease models [44–46]. Hepatic artery is the regional delivery route in liver disease. Actually, MSCs have been transplanted through the hepatic artery for the treatment of liver disease in clinic trials [19, 47]. Hepatic artery puncture is performed through femoral artery catheterization, which is less invasive than portal vein puncture. It is difficult to carry out hepatic artery puncture in small animals, such as mice. Therefore, the engraftment efficiency and therapy efficacy of MSCs delivered through these two routes need to be compared through large animal experiments or clinic trials in the future.

In conclusion, BLI, which could dynamically and quantitatively track cellular location and survival, is useful in determining MSCs transplantation parameters, such as delivery dose and route. However, further molecular imaging studies are needed to answer essential questions about clinical application of MSCs. BLI is limited to small animal studies due to its shallow penetration depth. The application of radionuclide reporter genes, such as herpes simplex virus type 1 thymidine kinase (HSV1-tk) or sodium iodide symporter (NIS), will facilitate large animal studies and clinical translation. Besides, the accurate cellular spatial localization information can be obtained through the incorporation of MRI reporter genes, such as Ferritin or lysine-rich protein (LRP). Former studies have confirmed the therapeutic effect of MSCs in acute liver injury [16, 23]. This study investigated MSCs delivery parameters exclusively on cell retention. Therefore, the relationship between cell retention and subsequent therapeutic efficacy needs to be further explored. MSCs are heterogeneous and contain subpopulations with different self-renewal and differentiation ability [48]. To date, little information is available to distinguish between individual subpopulations. The identification of MSCs subpopulations with favorable characteristics will facilitate specialized MSCs therapy in liver disease. Besides, some studies report tumorigenic potential of MSCs [49]. Thus, the safety of MSCs transplantation must be thoroughly observed especially when applied to premalignant liver disease. For a long time, MSCs were thought to be "immune privileged". However, recent studies indicate that allogeneic or xenogeneic transplanted MSCs can be immunogenic. Activated NK cells [50], memory T cells [51, 52],

macrophages [53, 54], and antidonor IgG [55] were reported to mediate the immune rejection of MSCs. In this study, the number of MSCs engrafted in the liver decreased progressively with time, and they were not detected at 10-day PT after SMV infusion. The liver is an organ of the immune system and contains abundant NK cells, macrophages, and lymphocytes [56, 57]. Therefore, it is crucial to elucidate the mechanism of the immune response against MSCs in the liver, which will further aid in the optimization of treatment strategy.

Acknowledgments. This work was supported by the National Natural Science Foundation of China (No. U1032002, 81271621, 81301266, 81101096) and Key Clinical Research Project of Public Health Ministry of China 2010–2012 (No. 164).

Conflict of Interest. The authors have declared that they have no conflict of interest.

Electronic supplementary material

Below is the link to the electronic supplementary material.ESM 1(PDF 2823 kb)

References

1. da Silva ML, Chagastelles PC, Nardi NB (2006) Mesenchymal stem cells reside in virtually all post-natal organs and tissues. J Cell Sci 119:2204–2213
2. Lee KD, Kuo TK, Whang-Peng J et al (2004) *In vitro* hepatic differentiation of human mesenchymal stem cells. Hepatology 40:1275–1284
3. Snykers S, Vanhaecke T, Papeleu P et al (2006) Sequential exposure to cytokines reflecting embryogenesis: the key for *in vitro* differentiation of adult bone marrow stem cells into functional hepatocyte-like cells. Toxicol Sci 94:330–341, discussion 235–339
4. Banas A, Teratani T, Yamamoto Y et al (2007) Adipose tissue-derived mesenchymal stem cells as a source of human hepatocytes. Hepatology 46:219–228
5. Chivu M, Dima SO, Stancu CI et al (2009) *In vitro* hepatic differentiation of human bone marrow mesenchymal stem cells under differential exposure to liver-specific factors. Transl Res 154:122–132
6. Yamazaki S, Miki K, Hasegawa K et al (2003) Sera from liver failure patients and a demethylating agent stimulate transdifferentiation of murine bone marrow cells into hepatocytes in coculture with nonparenchymal liver cells. J Hepatol 39:17–23
7. Qihao Z, Xigu C, Guanghui C, Weiwei Z (2007) Spheroid formation and differentiation into hepatocyte-like cells of rat mesenchymal stem cell induced by co-culture with liver cells. DNA Cell Biol 26:497–503
8. Deng X, Chen YX, Zhang X et al (2008) Hepatic stellate cells modulate the differentiation of bone marrow mesenchymal stem cells into hepatocyte-like cells. J Cell Physiol 217:138–144
9. Kazemnejad S, Allameh A, Soleimani M et al (2009) Biochemical and molecular characterization of hepatocyte-like cells derived from human bone marrow mesenchymal stem cells on a novel three-dimensional biocompatible nanofibrous scaffold. J Gastroenterol Hepatol 24:278–287
10. Ji R, Zhang N, You N et al (2012) The differentiation of MSCs into functional hepatocyte-like cells in a liver biomatrix scaffold and their transplantation into liver-fibrotic mice. Biomaterials 33:8995–9008
11. Ishii K, Yoshida Y, Akechi Y et al (2008) Hepatic differentiation of human bone marrow-derived mesenchymal stem cells by tetracycline-regulated hepatocyte nuclear factor 3beta. Hepatology 48:597–606
12. Sato Y, Araki H, Kato J et al (2005) Human mesenchymal stem cells xenografted directly to rat liver are differentiated into human hepatocytes without fusion. Blood 106:756–763
13. Kuo TK, Hung SP, Chuang CH, *et al.* (2008) Stem cell therapy for liver disease: parameters governing the success of using bone marrow mesenchymal stem cells. Gastroenterology 134: 2111–2121, 2121 e2111-2113.
14. Di Rocco G, Gentile A, Antonini A et al (2012) Analysis of biodistribution and engraftment into the liver of genetically modified mesenchymal stromal cells derived from adipose tissue. Cell Transplant 21:1997–2008
15. Parekkadan B, van Poll D, Suganuma K et al (2007) Mesenchymal stem cell-derived molecules reverse fulminant hepatic failure. PLoS One 2:e941
16. Banas A, Teratani T, Yamamoto Y et al (2008) IFATS collection: *in vivo* therapeutic potential of human adipose tissue mesenchymal stem cells after transplantation into mice with liver injury. Stem Cells 26:2705–2712
17. van Poll D, Parekkadan B, Cho CH et al (2008) Mesenchymal stem cell-derived molecules directly modulate hepatocellular death and regeneration *in vitro* and *in vivo*. Hepatology 47:1634–1643
18. Kharaziha P, Hellstrom PM, Noorinayer B et al (2009) Improvement of liver function in liver cirrhosis patients after autologous mesenchymal stem cell injection: a phase I-II clinical trial. Eur J Gastroenterol Hepatol 21:1199–1205
19. Peng L, Xie DY, Lin BL et al (2011) Autologous bone marrow mesenchymal stem cell transplantation in liver failure patients caused by hepatitis B: short-term and long-term outcomes. Hepatology 54:820–828
20. Zhou B, Shan H, Li D et al (2010) MR tracking of magnetically labeled mesenchymal stem cells in rats with liver fibrosis. Magn Reson Imaging 28:394–399
21. Yukawa H, Watanabe M, Kaji N et al (2012) Monitoring transplanted adipose tissue-derived stem cells combined with heparin in the liver by fluorescence imaging using quantum dots. Biomaterials 33:2177–2186
22. Gholamrezanezhad A, Mirpour S, Bagheri M et al (2011) *In vivo* tracking of 111In-oxine labeled mesenchymal stem cells following infusion in patients with advanced cirrhosis. Nucl Med Biol 38:961–967
23. Wu C, Li J, Pang P et al (2014) Polymeric vector-mediated gene transfection of MSCs for dual bioluminescent and MRI tracking *in vivo*. Biomaterials 35:8249–8260
24. Mori T, Kiyono T, Imabayashi H et al (2005) Combination of hTERT and bmi-1, E6, or E7 induces prolongation of the life span of bone marrow stromal cells from an elderly donor without affecting their neurogenic potential. Mol Cell Biol 25:5183–5195
25. Zhang B, Shan H, Li D et al (2012) The inhibitory effect of MSCs expressing TRAIL as a cellular delivery vehicle in combination with cisplatin on hepatocellular carcinoma. Cancer Biol Ther 13:1175–1184
26. Li D, Liu S, Liu R et al (2013) Targeting the EphB4 receptor for cancer diagnosis and therapy monitoring. Mol Pharm 10:329–336
27. Liu S, Li D, Park R et al (2013) PET imaging of colorectal and breast cancer by targeting EphB4 receptor with 64Cu-labeled hAb47 and hAb131 antibodies. J Nucl Med 54:1094–1100
28. Li D, Liu S, Liu R et al (2014) Axl-targeted cancer imaging with humanized antibody h173. Mol Imaging Biol 16:511–518
29. Gu E, Chen WY, Gu J et al (2012) Molecular imaging of stem cells: tracking survival, biodistribution, tumorigenicity, and immunogenicity. Theranostics 2:335–345
30. Nguyen PK, Riegler J, Wu JC (2014) Stem cell imaging: from bench to bedside. Cell Stem Cell 14:431–444
31. Shcherbo D, Murphy CS, Ermakova GV et al (2009) Far-red fluorescent tags for protein imaging in living tissues. Biochem J 418:567–574
32. Lee RH, Seo MJ, Pulin AA et al (2009) The CD34-like protein PODXL and alpha6-integrin (CD49f) identify early progenitor MSCs with increased clonogenicity and migration to infarcted heart in mice. Blood 113:816–826
33. Yukawa H, Noguchi H, Oishi K et al (2009) Cell transplantation of adipose tissue-derived stem cells in combination with heparin attenuated acute liver failure in mice. Cell Transplant 18:611–618
34. Manibusan MK, Odin M, Eastmond DA (2007) Postulated carbon tetrachloride mode of action: a review. J Environ Sci Health C Environ Carcinog Ecotoxicol Rev 25:185–209
35. Gao J, Dennis JE, Muzic RF et al (2001) The dynamic *in vivo* distribution of bone marrow-derived mesenchymal stem cells after infusion. Cells Tissues Organs 169:12–20
36. Schrepfer S, Deuse T, Reichenspurner H et al (2007) Stem cell transplantation: the lung barrier. Transplant Proc 39:573–576
37. Fischer UM, Harting MT, Jimenez F et al (2009) Pulmonary passage is a major obstacle for intravenous stem cell delivery: the pulmonary first-pass effect. Stem Cells Dev 18:683–692

38. Deak E, Ruster B, Keller L et al (2010) Suspension medium influences interaction of mesenchymal stromal cells with endothelium and pulmonary toxicity after transplantation in mice. Cytotherapy 12:260–264
39. Kerkela E, Hakkarainen T, Makela T et al (2013) Transient proteolytic modification of mesenchymal stromal cells increases lung clearance rate and targeting to injured tissue. Stem Cells Transl Med 2:510–520
40. Gregory CA, Ylostalo J, Prockop DJ (2005) Adult bone marrow stem/progenitor cells (MSCs) are preconditioned by microenvironmental "niches" in culture: a two-stage hypothesis for regulation of MSC fate. Sci STKE 2005:pe37
41. Breitbach M, Bostani T, Roell W et al (2007) Potential risks of bone marrow cell transplantation into infarcted hearts. Blood 110:1362–1369
42. am Esch JS 2nd, Knoefel WT, Klein M et al (2005) Portal application of autologous CD133+ bone marrow cells to the liver: a novel concept to support hepatic regeneration. Stem Cells 23:463–470
43. Lee RH, Pulin AA, Seo MJ et al (2009) Intravenous hMSCs improve myocardial infarction in mice because cells embolized in lung are activated to secrete the anti-inflammatory protein TSG-6. Cell Stem Cell 5:54–63
44. Ishizaka S, Horie N, Satoh K et al (2013) Intra-arterial cell transplantation provides timing-dependent cell distribution and functional recovery after stroke. Stroke 44:720–726
45. Huang Z, Shen Y, Pei N et al (2013) The effect of nonuniform magnetic targeting of intracoronary-delivering mesenchymal stem cells on coronary embolisation. Biomaterials 34:9905–9916
46. Cai J, Yu X, Xu R et al (2014) Maximum efficacy of mesenchymal stem cells in rat model of renal ischemia-reperfusion injury: renal artery administration with optimal numbers. PLoS One 9:e92347
47. Khan AA, Parveen N, Mahaboob VS et al (2008) Safety and efficacy of autologous bone marrow stem cell transplantation through hepatic artery for the treatment of chronic liver failure: a preliminary study. Transplant Proc 40:1140–1144
48. Harichandan A, Buhring HJ (2011) Prospective isolation of human MSC. Best Pract Res Clin Haematol 24:25–36
49. Meier RP, Muller YD, Morel P et al (2013) Transplantation of mesenchymal stem cells for the treatment of liver diseases, is there enough evidence? Stem Cell Res 11:1348–1364
50. Spaggiari GM, Capobianco A, Becchetti S et al (2006) Mesenchymal stem cell-natural killer cell interactions: evidence that activated NK cells are capable of killing MSCs, whereas MSCs can inhibit IL-2-induced NK-cell proliferation. Blood 107:1484–1490
51. Eliopoulos N, Stagg J, Lejeune L et al (2005) Allogeneic marrow stromal cells are immune rejected by MHC class I- and class II-mismatched recipient mice. Blood 106:4057–4065
52. Zangi L, Margalit R, Reich-Zeliger S et al (2009) Direct imaging of immune rejection and memory induction by allogeneic mesenchymal stromal cells. Stem Cells 27:2865–2874
53. Grinnemo KH, Mansson A, Dellgren G et al (2004) Xenoreactivity and engraftment of human mesenchymal stem cells transplanted into infarcted rat myocardium. J Thorac Cardiovasc Surg 127:1293–1300
54. Coyne TM, Marcus AJ, Woodbury D, Black IB (2006) Marrow stromal cells transplanted to the adult brain are rejected by an inflammatory response and transfer donor labels to host neurons and glia. Stem Cells 24:2483–2492
55. Poncelet AJ, Vercruysse J, Saliez A, Gianello P (2007) Although pig allogeneic mesenchymal stem cells are not immunogenic *in vitro*, intracardiac injection elicits an immune response *in vivo*. Transplantation 83:783–790
56. Bertolino P, Klimpel G, Lemon SM (2000) Hepatic inflammation and immunity: a summary of a conference on the function of the immune system within the liver. Hepatology 31:1374–1378
57. Mehal WZ, Azzaroli F, Crispe IN (2001) Immunology of the healthy liver: old questions and new insights. Gastroenterology 120:250–260